DOI: 10.21062/mft.2026.042 © 2026 Manufacturing Technology. All rights reserved. http://www.journalmt.com

The Effect of Accelerated Weathering on the Properties of Coatings on an Aluminium Substrate

Katarína Moricová (0000-0002-2465-5672)[1], Jana Šulcová (0000-0002-1148-2581)[1], Iveta Papučová (0000-0002-3626-4783)[1], Róbert Janík (0000-0002-4178-1865)[1], Aleksandra Ewa Nowicka (0000-0002-2572-7789)[2]
[1]Faculty of Industrial Technologies, Alexander Dubček University of Trenčín, I. Krasku 491/30, 020 01 Púchov, Slovak Republic. E-mail: katarina.moricova@tnuni.sk
[2]FunGlass – Centre for Functional and Surface Functionalized Glass, Alexander Dubcek University of Trenčín, Študentská 2, 911 50, Trenčín, Slovak Republic

Oxide coatings ZnO and TiO_2 are characterized by good chemical stability, non-toxicity, photocatalytic activity, and the potential to improve the corrosion resistance of underlying materials. The aim of this study is to prepare and evaluate these environmentally friendly coatings applied to an aluminium substrate, which is one of the most widely used technical metals. X-ray fluorescence spectrometry employed was used to determine the chemical composition. Surface properties were investigated by measuring the contact angle on samples before exposure to UV radiation and condensation, and after 98 and 196 hours of exposure in a UV chamber. The structure of the prepared samples was analysed using atomic force microscopy (AFM). Based on the obtained results, it can be concluded that plasma treatment of the aluminium substrates increases the surface free energy (SFE). However, after exposure to controlled UV radiation and condensation (196 hours), the hydrophilicity of the surface increases to approximately the same value for all prepared samples. Samples coated with ZnO were found to be less stable under the given conditions compared to TiO_2-coated samples and exhibited higher surface roughness.

Keywords: Contact angle, UV radiation, Aluminium substrate, Oxide coatings, Atomic force microscopy

1 Introduction

Aluminium is characterized by low density and good electrical and thermal conductivity. Its electrical conductivity reaches approximately 60% of that of copper while maintaining a significantly lower weight. This combination of properties enables its extensive use in electrical engineering, where it is employed in the production of conductors and cables, particularly in power distribution networks. In addition, aluminium exhibits high corrosion resistance and good reflectivity of light and heat, which further broadens its application in optical and thermal technologies [1-4].

One of the most important properties of aluminium is its ability to form a thin passive layer of aluminium oxide (Al_2O_3) on its surface. This layer forms spontaneously upon contact with oxygen in the atmosphere. The oxide film, typically several nanometers thick, is compact, chemically stable, and strongly adherent to the substrate. Owing to these properties, it effectively prevents further penetration of oxygen and moisture to the metal surface, thereby providing natural corrosion protection. This phenomenon, referred to as passivation, is a key factor contributing to the long service life of aluminium materials under atmospheric conditions [5,6].

From the perspective of surface engineering, aluminium is a suitable substrate for the application of functional coatings capable of significantly modifying its surface properties. Frequently used materials include titanium dioxide (TiO_2) and zinc oxide (ZnO), which are deposited as thin films using methods such as the sol–gel process, chemical vapor deposition (CVD), or physical vapor deposition (PVD). These materials possess specific physicochemical properties that improve the resistance of aluminium to degradation caused by ultraviolet radiation, moisture, and chemical agents [7-11].

Titanium dioxide is widely known for its photocatalytic activity, which enables the decomposition of organic compounds on the material surface under UV irradiation. This effect is utilized, for example, in the production of self-cleaning surfaces and in environmental applications for pollutant degradation. Zinc oxide exhibits similar properties while also demonstrating good antibacterial activity and high chemical stability. The application of these coatings may additionally alter the wettability of the surface, increasing either its hydrophilicity or hydrophobicity depending on the type of treatment. These surface modifications substantially expand the potential applications of aluminium in modern technologies [12-15]. The combination of its

favourable bulk properties and modified surface characteristics enables its use in areas where pure aluminium alone would be insufficient. Examples include building structures exposed to extreme conditions, functional surfaces with environmental significance, and components used in electrical engineering and nanotechnology [16-18].

The study investigatesd the effect of UV radiation and condensation on coated aliminium samples by means of surface free energy measurements, EDX analysis and AFM morphology evaluation.

2 Experimental

2.1 Preparation of sol

2.1.1 Preparation of TiO_2 sol

The following chemicals were used for the preparation of the TiO_2 sol: titanium isopropoxide (iPTi, 98%, Acros Organics) as the precursor, acetylacetone (AcAc, 99.5%, Penta) as the stabilizer, acetic acid (CH_3COOH, 99.0%, Centralchem) as the catalyst, isopropyl alcohol (IPA, 99.7%, Centralchem) as the solvent and distilled water. The preparation procedure consisted of two steps.

- Solution A: 22.9 cm³ of iPTi was gradually added dropwise to 40.8 cm³ of IPA in a plastic beaker under continuous stirring for approximately 4.5 minutes.
- Solution B: In a second beaker 7.9 cm³ of AcAc and 5.3 cm³ of distilled water were added to 40.8 cm³ of IPA under stirring. Subsequently 0.4 cm³ of CH_3COOH was added dropwise, while stirring continued for approximately 7 minutes.

The final sol was prepared by gradually adding Solution A to Solution B under continuous stirring for approximately 15 minutes. The resulting sol was then covered with a watch glass and stirred for an additional 2 hours.

2.1.2 Preparation of ZnO Sol

The following chemicals were used for the preparation of the ZnO sol: zinc acetate (ZnA, 99%, Centralchem) as the precursor, ethanol (EtOH, 99.8%, Centralchem) as the solvent and stabilizing medium, acetic acid (CH_3COOH, 99.0%, Centralchem) as the catalyst, distilled water.

A total of 4.38 g of ZnA and 100 cm³ of EtOH were added into a glass beaker and the mixture was stirred for 3 minutes at laboratory temperature. Subsequently, 4 cm³ of distilled water and 0.4 cm³ of CH_3COOH were added. The prepared solution was then stirred at 65 °C for 2 hours at a stirring speed of 210 rpm.

The molar composition of sols is shown in Table 1.

Tab. 1 *Molar composition of sols*

Sol	Component						
	iPTi	**AcAc**	**IPA**	**CH_3COOH**	**H_2O**	**ZnA**	**EtOH**
TiO_2	0.050	0.050	0.695	0.005	0.200	-	-
ZnO	-	-	-	0.004	0.115	0.010	0.868

2.2 Sample Preparation

Aluminium substrates were cut into dimensions of 2.5 × 7.5 cm and subsequently cleaned to remove surface impurities and contaminants. The cleaning procedure consisted of washing the substrates with a detergent, followed by rinsing with distilled water and IPA. After cleaning, the samples were dried in an oven at 60 °C for 1 h. A portion of the prepared substrates was further subjected to plasma treatment using a KPR 200 mm plasma reactor. The samples were placed into the reactor chamber and plasma was applied to both sides of the substrates at a power of 350 W for 10 s. The plasma treatment was carried out to activate the surface and improve the adhesion of subsequently deposited coatings.

Following the surface pre-treatment, TiO_2 and ZnO sols were deposited onto the aluminium substrates. The samples were immersed in the respective sol for 15 s and then withdrawn at a constant rate of 60 mm/min. After removal, the samples were held approximately 2 cm above the solution level for 2 min to ensure uniform solvent evaporation and stabilization of the formed coating. Following the deposition process, the coated samples were dried in an oven at 60 °C for 1 h and annealed at 450 °C for 1 h.

Based on the applied treatment and coating type, the following sample groups were prepared and assigned: Al cleaned, Al cleaned/TiO_2, Al cleaned/ZnO, Al plasma, Al plasma/TiO_2, and Al plasma/ZnO.

The prepared samples were exposed in a testing chamber QUV/Se LX-8047-TM for 98 h and 196 h under accelerated aging conditions. The exposure procedure consisted of alternating cycles of UVA irradiation and condensation, specifically 8 h of UVA radiation at 60 °C followed by 4 h of condensation at 50 °C.

2.3 Methods of characterisation

The sessile drop method was used to determine the contact angles of distilled water and diiodomethane on the investigated surfaces. For each substrate and coating, at least ten droplets of the test liquids distilled water (DW) and diiodomethane (DIM), each with a volume of 2 μL were deposited at different locations on the surface. The obtained contact angle values were statistically evaluated using the Grubbs test [19] for outlier detection, and identified outliers were excluded from the subsequent analysis of surface free energy. The measurements were performed using an Advance Drop Shape Analyzer (DSA30, Krüss). The free surface energy and its polar and dispersion components were calculated from the contact angle values using Owens-Wendt-Rabel-Kaelble (OWRK) method.

The morphology of the samples was investigated using a Bruker Inova® microscope. An RTE SPA-300 probe with a resonance frequency of approximately 300 kHz was employed for the measurements. Each sample was measured 6 to 10 times. The scanned area had dimensions of 20 × 20 μm. The obtained data were processed using NanoScope Analysis software (version 1.5), which enabled the evaluation of surface morphology, topography, and roughness parameters.

Semiquantitative chemical analysis of the substrates and deposited layers was performed using an EDX-7000 energy-dispersive X-ray fluorescence spectrometer (Shimadzu)

3 Results and discussion

3.1 Contact angle and surface free energy

The surface properties of the samples before exposure to UV radiation and condensation were evaluated by contact angle (CA) measurements. The surface free energy (SFE) was calculated from the contact angles of distilled water (CA DW) and diiodomethane (CA DIM). The obtained values are presented in Table 2. The lowest surface free energy was observed for the cleaned aluminium sample with a value of 54 mJ/m². After plasma treatment and coating deposition, the surface free energy increased to approximately 72 mJ/m².

Tab. 2 *Contact angle and surface energy values of the prepared samples before accelerated weathering tests*

Sample	CA DW (°)	CA DIM (°)	SFE (mJ/m²)	SFE dispersive component (mJ/m²)	SFE polar component (mJ/m²)
Al cleaned	60.14±3.38	35.40±1.62	53.44±2.55	41.84±0.76	11.60±1.80
Al plasma	39.48±3.58	37.63±1.93	64.36±2.95	40.78±0.93	23.58±2.02
Al cleaned/TiO_2	25.41±1.05	30.78±1.97	72.72±1.45	43.90±0.83	28.83±0.62
Al plasma/TiO_2	25.35±0.86	32.53±1.57	72.15±1.21	43.14±0.69	29.01±0.52
Al cleaned/ZnO	21.30±3.16	34.84±3.01	73.50±2.77	42.12±1.39	31.40±1.39
Al plasma/ZnO	26.65±1.25	37.44±1.78	70.82±1.59	40.88±0.86	29.95±0.73

After 98 h of exposure to UV radiation and condensation, the surface free energy values increased for all prepared samples (Table 3). The combined effect of moisture and UV radiation led to increased wettability and hydrophilicity of the surface. The increase in SFE suggests the formation of additional hydroxyl groups and oxidized surface species during UV ageing, which promoted stronger interactions with polar liquids and consequently reduced the contact angle [21,22].

Tab. 3 *Contact angle and surface energy values of the prepared samples after 98 hours of exposure in the UV chamber*

Sample	CA DW (°)	CA DIM (°)	SFE (mJ/m²)	SFE dispersive component (mJ/m²)	SFE polar component (mJ/m²)
Al cleaned 98h	31.85±10.97	32.10±9.97	69.57±10.06	43.33±4.34	26.24±5.72
Al plasma 98h	7.27±2.12	19.01±3.56	79.66±1.60	48.07±1.00	31.59±0.59
Al cleaned/TiO_2 98h	9.74±1.25	32.05±3.53	76.99±2.51	42.91±1.57	34.08±0.94
Al plasma/TiO_2 98h	5.89±1.40	8.81±2.74	80.84±0.61	50.20±0.37	30.63±0.24
Al cleaned/ZnO 98h	11.10±3.39	9.17±2.39	80.06±0.99	50.15±0.34	29.90±0.66
Al plasma/ZnO 98h	13.55±3.82	6.03±0.96	79.73±0.95	50.52±0.09	29.22±0.86

Tab. 4 *Contact angle and surface energy values of the prepared samples after 196 hours of exposure in the UV chambre*

Sample	CA DW (°)	CA DIM (°)	SFE (mJ/m²)	SFE dispersive component (mJ/m²)	SFE polar component (mJ/m²)
Al cleaned 196h	5.32±2.53	5.07±0.55	81.09±0.27	50.67±0.04	30.48±0.23
Al plasma 196h	6.84±3.26	4.33±0.90	80.96±0.44	50.66±0.06	30.30±0.38
Al cleaned/TiO_2 196h	3.29±1.82	5.30±2.40	81.23±0.34	50.58±0.20	30.64±0.14
Al plasma/TiO_2 196h	5.05±5.29	3.86±2.70	81.15±0.62	50.68±0.16	30.47±0.46
Al cleaned/ZnO 196h	6.59±2.30	5.52±2.22	80.94±0.46	50.56±0.19	30.37±0.28
Al plasma/ZnO 196h	16.46±15.61	8.53±2.05	78.87±4.88	50.24±0.27	28.63±4.21

After 196 h of exposure to UV radiation and condensation, the surface free energy values stabilized for all samples at approximately 81 mJ/m² (Table 4).

The observed changes in surface free energy can be attributed to the combined effects of UV radiation and condensation processes acting on the sample surfaces. UV irradiation promotes photo-oxidation reactions and the formation of new polar functional groups, particularly hydroxyl (–OH) groups, thereby increasing the polarity of the surface. Simultaneously, the condensation cycles ensure continuous exposure to moisture, which further enhances surface hydroxylation. These physicochemical changes lead to improved wettability and increased hydrophilicity, resulting in higher surface free energy values. In TiO_2 and ZnO coated samples, UV exposure additionally activation photocatalytic processes associated with the generation of reactive oxygen species and the subsequent formation of hydroxyl groups on the surface. These effects contribute to a further increase in the polar component of the surface free energy. However, during prolonged exposure to UV radiation, all investigated surfaces gradually underwent similar oxidation and hydroxylation processes induced by the combined action of UV radiation, oxygen, and moisture. Consequently, the differences between the individual surface modifications were gradually reduced with increasing exposure time.

3.2 AFM analysis and roughness

AFM 2D and 3D images (Figs. 1–3) revealed the presence of elongated groove-like structures on the surface, which can be attributed with the original mechanical processing and rolling direction of the aluminium substrate. The Al cleaned sample exhibited a relatively heterogeneous morphology characterized by pronounced height variations and distinct surface irregularities. Localized protrusions and depressions were observed, indicating increased surface roughness (Table 5) and non-uniform distribution of the surface layer.

The Al plasma/TiO_2 sample (Fig. 2) exhibited a smoother and more homogeneous surface morphology compared to the cleaned Al substrate. Although the groove-like topographical features remained visible, the height variations were less pronounced and the surface appeared more compact and uniform, without significant agglomeration or large defects. The homogeneous morphology indicates good adhesion of the TiO_2 coating and uniform coverage of the substrate surface [23].

In contrast, the Al plasma/ZnO sample (Fig. 3) exhibited a more heterogeneous and coarser surface morphology characterized by larger rounded formations and agglomerate-like structures. Pronounced protrusions were observed on the surface, which can be attributed to partial clustering of ZnO particles during the coating formation process. During drying and subsequent thermal treatment, crystal growth and particle aggregation likely occurred, resulting in the formation of a less uniform surface structure. The increased height variations and irregular surface texture indicate higher surface roughness (Table 5) and lower compactness in comparison with the TiO_2 coating [24,25].

Overall, the TiO_2 coating exhibited a more compact, homogeneous, and fine-grained morphology, whereas the ZnO coating showed a more granular, agglomerated, and heterogeneous surface structure.

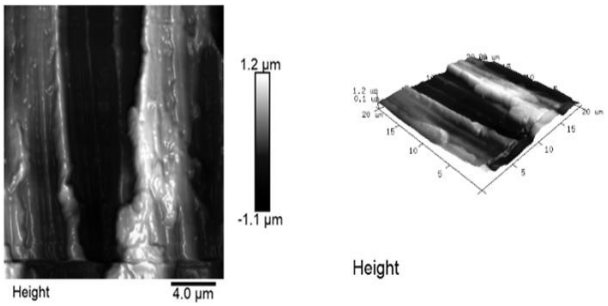


Fig. 1 *2D and 3D images of the surface of sample Al cleaned*

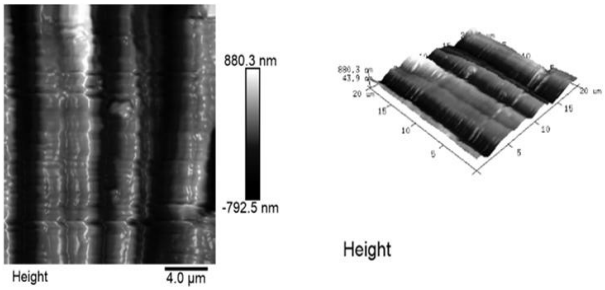


Fig. 2 *2D and 3D images of the surface of sample Al plasma/TiO_2*

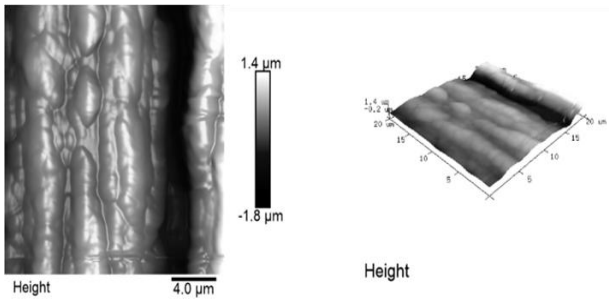


Fig. 3 *2D and 3D images of the surface of sample Al plasma/ZnO*

AFM analysis was also employed to determine the surface roughness parameters of the investigated samples (Table 5). The lowest values of Ra and Rq were observed for the Al plasma/TiO_2 sample. These results indicateing the formation of a relatively smooth and homogeneous coating, which is consistent with the surface morphology observed in the AFM images. In contrast, the ZnO-coated sample exhibited higher roughness values than the cleaned aluminium substrate. This behaviour may be attributed to the crystalline nature of ZnO and its growth mechanism during coating formation. ZnO typically tends to grow in a columnar morphology, forming elongated grains with pronounced peaks and valleys on the surface. Such structural features contribute to increased surface roughness, as reflected by the higher *Ra* and *Rq* values. The elevated roughness of the ZnO coating is further supported by the AFM observations, which revealed a more heterogeneous surface characterized by agglomerated structures and greater height variations compared to the TiO_2 coating.

Tab. 5 *Mean Ra-roughness and Rq-roughness values of surface of samples*

	Rq (nm)	Ra (nm)
Al cleaned	174.85±92.72	138.80±73.00
Al plasma/TiO_2	124.20±40.94	98.60±32.91
Al plasma/ZnO	194.60±66.23	156.80±61.48

3.3 Elemental analysis

Elemental composition of the prepared samples was analysed by energy-dispersive X-ray spectroscopy (EDX) (Table 6). The obtained results confirmed the presence of titanium and zinc in the coatings prepared from TiO_2 and ZnO sols, respectively. The detection of these elements verifies the successful deposition of the corresponding oxide layers onto the aluminium substrate.

Tab. 6 *Elemental composition of prepared samples*

	Al (wt.%)	Fe (wt.%)	Mn (wt.%)	Zn (wt.%)	Ti (wt.%)
Al cleaned	99.45±0.47	0.37±0.01	0.04±0.01	0.02±0.01	0.02±0.01
Al plasma	99.33±0.48	0.41±0.01	0.07±0.01	-	0.02±0.01
Al cleaned/TiO_2	98.78±0.49	0.40±0.01	0.05±0.01	-	0.62±0.01
Al plasma/TiO_2	98.62±0.49	0.44±0.01	0.05±0.01	0.02±0.01	0.67±0.01
Al cleaned/ZnO	99.311±0.46	0.38±0.01	0.05±0.01	0.05±0.01	-
Al plasma/ZnO	99.40±0.46	0.38±0.01	0.04±0.01	0.05±0.01	0.02±0.01

After 98 h of exposure to controlled UV radiation and condensation, a slight increase in the detected Ti and Zn contents was observed in the coated samples (Table 7). This increase is most likely attributable to the inherent measurement uncertainties and limitations of the EDX technique, particularly when quantifying elements present at relatively low concentrations. Therefore, the observed differences cannot be considered statistically significant and do not indicate substantial changes in the chemical composition of the deposited coatings.

Tab. 7 *Elemental composition of prepared samples after 98 hours in the UV chamber*

	Al (wt.%)	Fe (wt.%)	Mn (wt.%)	Zn (wt.%)	Ti (wt.%)
Al cleaned 98h	98.96±0.56	0.58±0.01	0.08±0.01	-	0.02±0.01
Al plasma 98h	99.11±0.55	0.56±0.01	0.08±0.01	0.03±0.01	-
Al cleaned/TiO_2 98h	98.56±0.53	0.50±0.00	0.06±0.01	0.02±0.01	0.75±0.01
Al plasma/TiO_2 98h	98.45±0.54	0.59±0.00	0.06±0.01	0.02±0.01	0.75±0.01
Al cleaned/ZnO 98h	98.98±0.54	0.55±0.01	0.06±0.01	0.07±0.01	0.02±0.01
Al plasma/ZnO 98h	98.96±0.55	0.58±0.01	0.07±0.01	0.07±0.01	-

After 196 h of exposure in the testing chamber, the detected concentrations of Ti and Zn remained essentially unchanged compared to those measured after 98 h of exposure (Table 8).

Tab. 8 *Elemental composition of prepared samples after 196 hours in the UV chamber*

	Al (wt.%)	Fe (wt.%)	Mn (wt.%)	Zn (wt.%)	Ti (wt.%)
Al cleaned 196h	99.13±0.56	0.57±0.01	0.06±0.01	0.03±0.01	0.02±0.01
Al plasma 196h	99.89±0.56	0.58±0.01	0.09±0.01	-	0.02±0.01
Al cleaned/TiO_2 196h	98.49±0.53	0.51±0.01	0.06±0.01	0.02±0.01	0.74±0.01
Al plasma/TiO_2 196h	98.23±0.55	0.53±0.01	0.06±0.01	0.03±0.01	0.82±0.01
Al cleaned/ZnO 196h	99.06±0.55	0.56±0.01	0.07±0.01	0.07±0.01	0.02±0.01
Al plasma/ZnO 196h	99.01±0.57	0.63±0.01	0.07±0.01	0.09±0.01	0.03±0.01

These results indicate that the TiO_2 and ZnO coatings retained their chemical composition throughout the accelerated weathering test and did not undergo significant degradation or loss of material. Therefore, the deposited layers can be considered stable and resistant to the combined effects of UV radiation and condensation, demonstrating good durability under the applied aging conditions.

4 Conclusion

This study was focused on investigating the influence of accelerated weathering conditions on the properties of TiO_2 and ZnO coatings deposited on an aluminium substrate. Surface activation by plasma treatment resulted in an increase in surface free energy, enhanced hydrophilicity, improved wettability, and the creation of favourable conditions for improved coating adhesion (for the deposition of uniform coatings). EDX analysis confirmed the presence of titanium and zinc containing surface layers even after exposure of the samples to accelerated weathering conditions, demonstrating their good chemical stability.

The TiO_2 coatings contributed to surface smoothing and a reduction in roughness parameters, whereas the ZnO coatings exhibited higher roughness due to their characteristic crystalline morphology and growth mechanism. AFM analysis revealed that the TiO_2 layer formed a more compact, homogeneous, and finer and more homogeneous structure, while the ZnO layer was characterized by a more heterogeneous and agglomerated surface morphology.

The combination of plasma surface treatment and TiO_2 coating deposition proved to be an effective approach for modifying the surface properties of aluminium. These findings have considerable practical potential, particularly in applications requiring enhanced surface wettability, coating uniformity, and long-term stability of surface coatings under environmental exposure conditions.

Acknowledgement

This work was supported by the Slovak Republic Grant Agency under the KEGA project 009TnUAD-4/2026

References

[1] CALLISTER, W. D., RETHWISCH, D. G. (2014). *Materials Science and Engineering: An Introduction*. 9th ed. Hoboken: Wiley, ISBN 978-1-118-32457-8.

[2] POLMEAR, I. J. (2005). *Light Alloys: From Traditional Alloys to Nanocrystals*, 4th ed. Oxford: Butterworth-Heinemann, ISBN 978-0-7506-6371-7.

[3] ZUPANIČ, F. et al. (2021). *Structure and Properties of Aluminium Alloys,* Basel: MDPI, ISBN 978-3-0365-1008-8.

[4] VARGEL, C. (2020). *Corrosion of Aluminium*. 2nd ed. Oxford: Elsevier, ISBN 978-0-08-099925-8.

[5] MIKUŠ, P., BREZNICKÁ, A., KOHUTIAR, M., et al. (2025), Experimental investigation of the effect of fuel on engine oil life. In: *Manufacturing Technology*, Vol. 25, No. 5, pp. 655-661, DOI: 10.21062/mft.2025.068.

[6] ĆURKOVIĆ, L., ĆURKOVIĆ, H., SPILLER, S., RENJO, M., ŠEGOTA, S. (2013). Enhancement of corrosion protection of AISI 304 stainless steel by nanostructured sol-gel TiO_2 films. In: *Corrosion Science*, Vol. 77, pp. 176-184, DOI:10.1016/j.corsci.2013.07.045

[7] KUZNETSOV, Y. I., REDKINA, G. V. (2022). Thin Protective Coatings on Metals Formed by Organic Corrosion Inhibitors in Neutral Media. In: *Coatings*, Vol. 12, No. 2, DOI: 10.3390/coatings12020149.

[8] AWANG, M., KHALILI, A. A., PEDAPATI, S. R. (2020). A Review: Thin Protective Coating for Wear Protection in High-Temperature Application. In: *Metals*, Vol. 10, No. 42, DOI: 10.3390/met10010042.

[9] ŠULCOVÁ, J., PAPUČOVÁ, I., et al. (2024). The Effect of TiO_2 Layers on the Surface Properties of Materials. In: *Manufacturing Technology*, Vol. 24, No. 2, pp. 272-278, DOI: 10.21062/mft.2024.022.

[10] METROKE, T.L., PARHHILL, R.L., KNOBBE, E.T. (2011). Passivation of metal alloys using sol–gel-derived materials-review. In: *Progress in Organic Coating*, Vol. 41, pp. 233-238, DOI:10.1016/S0300-9440(01)00134-5

[11] HAMID, M.A., RAHMAN, I. A. (2003). Preparation of titanium dioxide (TiO_2) thin films by sol gel dip coating method. In: *Malaysian Journal of Chemistry,* Vol. 5, pp. 86-91.

[12] CUAO MOREU, C. A. et al. (2026). Plasma-Driven Surface Functionalization: Enhancing the Corrosion Resistance of Aluminium via Atmospheric-Pressure Treatment. In: *Materials*, Vol. 19, No. 973, DOI: 10.3390/ma19050973

[13] JANÍK, R., LABAJ, I., SKALKOVÁ, P., ĎURIŠOVÁ, S., MORICOVÁ, K., (2024). Effects of Filler Modification on the Properties of Elastomeric Composites, In: *Manufacturing Technology*, Vol. 24, No. 3, pp. 365-377, DOI:10.21062/mft.2024.056.

[14] BAKOŠOVÁ, D., BAKOŠOVÁ, A. (2021). Analysis of Homogeneity and Young's Moduli of Rubber Compounds by Atomic Force Microscopy. In: *Manufacturing Technology*, Vol. 21, No. 6, pp. 749-756, DOI: 10.21062/mft.2021.099.

[15] TSAI, D. C. et al (2023). Influence of Plasma Treatment on Surface Characteristics of Aluminum Alloy Sheets and Bonding Performance of Composites. In: *Materials*, Vol.16, 3317. DOI: 10.3390/ma16093317.

[16] BINDER, W. H., SPERLING, E. (2021). Recent Developments in Surface Morphology Characterization of Functional Materials. In: *Surface and Interface Analysis*, Vol. 53, pp. 305–324. DOI: 10.1002/sia.6931.

[17] LI, C., WANG, Z., YANG, J. (2024). Surface Morphology Evolution in Plasma-Treated Metals. In: *Journal of Materials Science and Technology*, Vol. 105, pp. 152–162. DOI: 10.1016/j.jmst.2023.10.016.

[18] LEACH, R. (2013). *Characterisation of Areal Surface Texture*. Berlin: Springer, ISBN 978-3-642-36458-7.

[19] ECKSCHLAGER, K., HORSÁK, I., KODEJŠ, Z. (1980). *Vyhodnocování analytických výsledků a metod*. 1. vyd. Praha: SNTL, s.51.

[20] MUÑOZ, J., RINCÓN, R., CALZADA, M.D. (2019). Spatial Distribution of Wettability in Aluminum Surfaces Treated with an Atmospheric-Pressure Remote-Plasm*a.* In: *Metals*, Vol. 9, pp. 937. DOI: 10.3390/met9090937.

[21] MA, C., NIKIFOROV, A.; HEGEMANN, D., DE GEYTER, N., MORENT, R., OSTRIKOV, K. (2022). Plasma-controlled surface wettability: recent advances and future applications. In: *International Materials Reviews*, Vol. 68, No. 7, pp. 1-38. DOI:10.1080/09506608.2022.2047420.

[22] CHEN, X.; SELLONI, A. (2014). Titanium Dioxide (TiO_2) Nanomaterials. In: *Chemical Reviews*. Vol. 114, No. 19.

[23] XIAODONG, W, GUANGMING, W., et al. (2013). Optical Constants of Crystallized TiO_2 Coatings Prepared by Sol-Gel Process. In. *Materials*. Vol. 6, pp. 2819-2830, DOI:10.3390/ma6072819.

[24] JITAO, Z., WILLIAMS, G., THANAPHUN, J., et al. (2024). Wettability and Bactericidal Properties of Bioinspired ZnO Nanopillar Surfaces. In: *Langmuir*. Vol. 40, No. 14, pp. 7353-7363, DOI: 10.1021/acs.langmuir.3c03537.

[25] BINGYAO, D., XIONG, Y., QUFU, W., WEIDONG, G., (2007) AFM characterization of nonwoven material functionalized by ZnO sputter coating. In**:** *Materials Characterization*. Vol. 58, pp. 854–858.